



ORIGINAL PAPER

MINERALOGICAL AND TEXTURAL CONTROLS ON THE MECHANICAL BEHAVIOR OF SANDSTONES FROM THE NIZAMPUR AND KOHAT BASINS, PAKISTAN

Sajjad AHMAD¹*, Muhammad Tahir SHAH¹, Muhammad SAJID^{2,3}, Abdul Rahim ASIF^{1,4}*, Subhan ULLAH^{1,5}, Muhammad RIZWAN⁶, Syed Irfanullah HASHMI⁷, Shehzad MUSSAWAR⁸, Syed Saddam HUSSAIN⁹ and Hafiz Shahid HUSSAIN¹⁰

¹*National Centre of Excellence in Geology, University of Peshawar, Peshawar 25120, Pakistan*

²*Department of Geology, University of Peshawar, Peshawar 25120, Pakistan*

³*Department of Geology, Abdul Wali Khan University Mardan, Mardan 23200, Pakistan*

⁴*Department of Earth Sciences, Fata University, FR Kohat 26100, Pakistan*

⁵*Centre for Earth and Space Sciences, University of Swat, Swat 19120, Pakistan*

⁶*State Key Laboratory of Continental Evolution and Early Life, Department of Geology, Northwest University, Xi'an 710069, China*

⁷*Energy & Power Department, Government of Khyber Pakhtunkhwa, Peshawar 25000, Pakistan*

⁸*CECOS University of IT and Emerging Sciences, Peshawar, Peshawar 25000, Pakistan*

⁹*School of Sciences, University of Wollongong, 2500 Wollongong, Australia*

¹⁰*Macquarie University, Balaclava Rd, Macquarie Park NSW 2113, Australia*

*Corresponding author's e-mail: sajjadahmadshagai@gmail.com; abduhrahimasif@uop.edu.pk

ARTICLE INFO**Article history:**

Received 5 August 2025

Accepted 20 October 2025

Available online 5 November 2025

Keywords:

Sandstone

Mineralogy

Mechanical properties

Quartz-to-feldspar ratio

Geotechnical characterization,

Pakistan

ABSTRACT

Sandstone is a widely used construction material, with its mechanical behavior strongly influenced by mineralogical composition and textural characteristics. This study investigates these factors in sandstones from the Nizampur and Kohat basins in Pakistan through petrographic analysis, scanning electron microscopy (SEM), energy-dispersive X-ray spectroscopy (EDS), and geotechnical testing. Results reveal a strong positive correlation between quartz content and mechanical properties, including unconfined compressive strength (UCS), tensile strength (UTS), and point load index (PLT). The quartz-rich sandstone (quartz arenite) of the Lumshiwai Formation exhibited the highest strength (UCS: 145 MPa, UTS: 19 MPa), while the feldspathic litharenite of the Nagri Formation showed the weakest performance (UCS: 63 MPa, UTS: 5 MPa) due to poor sorting, high porosity, and compositional immaturity. Textural analysis demonstrated that tightly packed grains with straight, concavo-convex, and sutured contacts enhance strength, whereas poor sorting and high porosity reduce it. Non-destructive tests, such as Schmidt hammer (SHT) and ultrasonic pulse velocity (UPV), correlated well with quartz content, providing practical field assessment tools. This study reveals that quartz content alone can predict over 94 % of the variation in the compressive strength of sandstones from the Nizampur and Kohat basins. These findings highlight the critical role of mineralogy and texture in determining sandstone strength, offering valuable insights for construction and geotechnical applications. This study bridges a significant knowledge gap on sandstones from Pakistan, contributing to improved engineering practices.

1. INTRODUCTION

Sandstone, one of the most common sedimentary rocks, is extensively used in geotechnical and engineering applications. The physical and mechanical properties of sandstone are significantly influenced by its mineralogical composition and textural characteristics. Understanding these relationships is crucial for evaluating the suitability of sandstone in various construction projects (Naseer et al., 2019; Heydarian et al., 2024). Ahmad et al. (2021) investigated the mineralogical and textural influence on the physico-mechanical properties of granitoids from the Besham Syntaxes, northern Pakistan. Their study revealed that textural characteristics and mineralogy, including the modal percentage of minerals, degree of alteration, recrystallization, grain size and shape, and types of grain boundary contacts, have a significant impact on the physico-mechanical properties of the rocks. Ullah et al. (2025) demonstrate that textural variations in limestones play a critical role

in determining their geomechanical behavior, with strength properties varying across different limestone types. The mineralogical composition of sandstone, particularly the content of quartz and feldspar, plays a pivotal role in determining its strength and durability. Quartz, characterized by strong covalent bonds and high elastic stiffness, is a primary contributor to the strength of sandstone (Tuğrul and Zarif, 1999; Yesiloglu-Gultekin et al., 2013; Zhang et al., 2025). A strong positive correlation exists between quartz content and mechanical properties such as unconfined compressive and tensile strength (Sajid and Arif, 2015). Conversely, feldspar content reduces rock strength due to its inherent brittleness, cleavage planes, and susceptibility to alteration (Hemmati et al., 2020). The quartz-to-feldspar ratio (QFR) generally positively correlates with rock strength, with higher QFR values indicating more robust mechanical performance (Asif et al., 2024; Yusof and Zabidi, 2016).

Textural properties, including grain size, shape, degree of interlocking, porosity, and cementation, further modify the mechanical behavior of sandstone. Rocks with well-interlocked grains and silica cement exhibit higher strength and resistance to wear, while those with clay or calcareous cement are weaker (Shakoor and Bonelli, 1991; Tamrakar et al., 2007). Porosity is a significant factor, as higher porosity facilitates the initiation and propagation of cracks under loading, thereby reducing strength (Ozturk et al., 2014; Nawaz et al., 2025a, b). Additionally, diagenetic processes such as compaction, cementation, and pressure solution influence the textural characteristics and mechanical behavior of sandstone (Yasin, 2017).

Previous studies have established quantitative relationships between mineralogical and textural characteristics and mechanical properties of sandstone. For instance, multiple regression analyses have revealed that quartz content exerts the highest influence on UCS, followed by the QFR and feldspar content (Hemmati et al., 2020). Similarly, the type of cementation significantly impacts the strength and durability of sandstone, with siliceous cementation leading to more robust mechanical properties compared to clay or calcareous cementation (Wang et al., 2025). The mechanical properties of rock material are significantly influenced by its mineralogical properties (Asif et al., 2025; Nawaz et al., 2025c, d; Waqar et al., 2025). Strong rocks are generally those with siliceous cement, followed by calcite and iron minerals (such as hematite and chromite), while those with clay and phyllosilicate (such as mica) cement are weak. Several authors have investigated the relationship between mineralogical composition and the geomechanical properties of different rock types. Recently, researchers have paid increasing attention to the application of simulation methods to predict the behavior of rock containing different mineralogical compositions (Askaripour et al., 2022). The present study aims to explore the mineralogical and textural influences on the physical and mechanical properties of selected sandstones from Pakistan. By integrating petrographic, physical, and mechanical analyses, this research seeks to provide a comprehensive understanding of the factors governing the engineering behavior of sandstone, offering valuable implications for construction and geotechnical applications. Despite the widespread occurrence and economic significance of sandstone formations in Pakistan, a comprehensive study linking their detailed mineralogical and textural characteristics to their geomechanical properties has been lacking. This research aims to bridge this critical gap by providing a foundational dataset and establishing correlations that enhance the understanding of the engineering potential of sandstones in the region.

2. GENERAL GEOLOGY OF THE STUDY AREA

In Pakistan, sandstone formations occur in diverse geological settings, particularly within the

Nizampur and Kohat basins (Fig. 1). These formations, ranging in age from Eocene to Miocene, predominantly consist of feldspathic and quartzose sandstones (Shah, 2009). A prominent Cretaceous unit in Nizampur is the Chichali Formation (Early Cretaceous), which consists mainly of dark grey to green glauconitic shale with minor thin sandstones. The Chichali Formation represents an offshore marine shelf environment – its glauconite and marine fossils indicate a transgressive phase in the early Cretaceous. Above the shales, the deposition shifted to clastics with the Lumshiwai Formation. The Lumshiwai Formation is dominantly a sandstone unit: medium- to coarse-grained, greenish-gray sandstone with occasional interbedded shales. It often contains glauconite and marine fossils, signifying a shallow marine to nearshore setting (possibly a shoreface or deltaic environment) (Hashmi et al., 2018). The stratigraphic framework of Nizampur Basin from oldest to youngest is: Samana Suk Formation (Jurassic limestone) – Chichali Formation (Lower Cretaceous shale) – Lumshiwai Formation (Cretaceous sandstone) – Kawagarh Formation (Upper Cretaceous limestone) – Hangu Formation (Paleocene sandstone) – Lockhart Limestone (Paleocene) – Patala Formation (Paleocene shale) – Margalla Hill (Sakesar) Limestone (Early Eocene). This entire sequence has been deformed by thrust faults (notably the Kahi Thrusts in the area) which repeat and juxtapose various sections (Yaseen et al., 2021). The overall Cretaceous stratigraphy of Nizampur thus reflects a transgressive–regressive cycle: marine shale (Chichali) to shoreline sandstone (Lumshiwai) to marine limestone (Kawagarh).

The Kohat Basin contains a slightly broader stratigraphic range than Nizampur, including not only Mesozoic and Paleogene units (often exposed in the surrounding ranges), but also a thick sequence of Neogene molasse (which is largely missing in Nizampur). The Neogene molasse sequence in the Kohat Basin is very well developed, recording the influx of clastic sediments eroded from the rising Himalayas. The basal part of this molasse is the Murree Formation. The sandstones in the Murree Formation are typically fine- to medium-grained, pinkish or brown. Sedimentologically, the Murree Formation represents alluvial fan to fluvial over bank deposits laid down in an underfilled foreland basin setting; paleocurrent studies suggest sediment transport from north and northeast (from the rising Himalayas). The Nagri Formation (Late Miocene, ~11–9 Ma) lies above Chinji and marks an increase in grain size and sand content. It is dominated by thick-bedded, medium- to coarse-grained sandstones (commonly yellowish or brown) with subordinate reddish mudstone. The Nagri sandstones often represent broad, multi-storied channel belt deposits of large rivers in the foreland. These are laterally extensive and form prominent ridges and cuestas. The Nagri Formation in Kohat may be up to 1000–1500 m thick (Meissner et al., 1974).

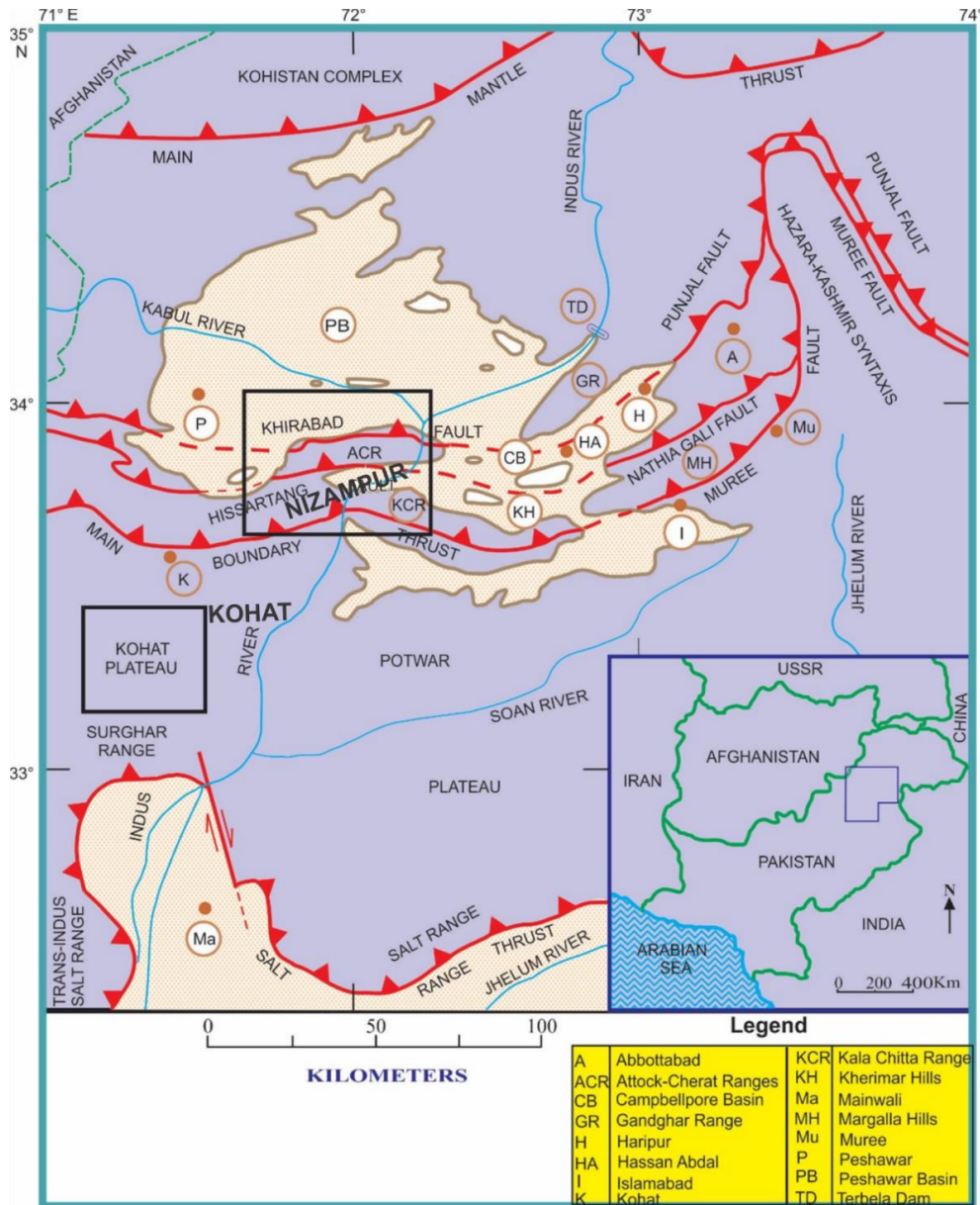


Fig. 1 Tectonic map of northern Pakistan showing major structural boundaries (after Hylland and Riaz, 1988). The study area (Nizampur and Kohat basins) has been shown as a box in the map.

Despite their economic significance as construction materials and their role in reconstructing the tectonic and sedimentary history of northern Pakistan, the relationship between their mineralogical and textural attributes and mechanical properties remains poorly understood.

3. MATERIAL AND METHODS

3.1. FIELDWORK

A comprehensive field work was conducted in the Nizampur and Kohat basins and a total of 25 bulk samples (5 for each Sandstone variety) were collected from selected sandstone formations (Fig. 2). The studied formations were chosen because they are among the most extensively exposed and widely utilized sandstone units in the region for construction and aggregate purposes. Furthermore, they represent

a broad range of compositional and textural characteristics, from quartz arenites to feldspathic litharenites, making them ideal for investigating the influence of these variables on physical and mechanical properties.

For the collection of bulk samples, several careful sampling techniques were employed to ensure that the material was representative and free from weathering influences. Fresh outcrop sampling was prioritized, with samples being taken from unweathered surfaces to reflect the true geological and mechanical properties of the samples. In areas where deeper samples were needed, core drilling was conducted to extract material beneath the weathered layers. Where drilling was not feasible, chiseling was used to collect fresh rock samples from below the weathered surface. Additionally, small trenches were



Fig. 2 Field Photographs of the studied formations from the Nizampur and Kohat Basins, Pakistan. **A)** Murree Formation in the Kohat Basin, **B)** Chichali Formation in the Nizampur Basin, **C)** Lumshiwal Formation in the Nizampur Basin and **D)** Nagri Formation in the Kohat Basin.

dug around the outcrops to expose fresh rock for sampling. Large blocks were also cut from selected areas to ensure that sufficient material was available for analysis. After collection, all samples were carefully sealed and stored to prevent contamination or moisture absorption, maintaining their integrity for testing. These methods ensured that the bulk samples represented the actual in-situ conditions of the formations.

3.2. LABORATORY WORK

Petrographic Analysis:

The thin sections were prepared in the rock-cutting laboratory, National Centre of Excellence in Geology (NCEG), University of Peshawar (UoP), KP, Pakistan, for petrographic analysis. The thin sections were studied using a Nikon ECLIPSE LV100ND polarizing microscope. During the petrographic analysis, the mineralogical and textural characteristics of the investigated samples were observed, and photomicrographs were captured using a Nikon DS-Fi2 camera that was connected to the microscope.

SEM and EDS Analysis:

The collected samples were analyzed using Scanning Electron Microscopy (SEM) and Energy-Dispersive X-ray Spectroscopy (EDS) to reveal textural and mineralogical variations. A JEOL JSM-IT-100 SEM at NCEG, UoP, was utilized, employing both scanning and back-scattered modes for detailed imaging and comprehensive mineralogical and textural characterization.

Geotechnical analysis:

Cylindrical cores were extracted from the bulk samples at the Geotechnical Laboratory of the NCEG, UOP, to analyze the geotechnical behavior of the studied formations (Fig. 3). Each sample was drilled with a core that had a diameter of at least 50 mm and a length-to-diameter ratio (L/D) of 2.0–2.5 (ASTM D-4543-19). All laboratory tests were conducted following specific standards, which are detailed in Table 1. Porosity was calculated indirectly using the values of specific gravity and water absorption. The testing methodologies adhered to internationally recognized standards, including the American Society for Testing and Materials (ASTM). The ASTM standards provide precise guidelines for evaluating the mechanical and physical properties of rocks, ensuring consistency across geotechnical and construction studies.

4. RESULTS

4.1. PETROGRAPHIC, SEM, AND EDS ANALYSES

A detailed petrographic analysis of the four sandstone formations (i.e., Chichali, Lumshiwal, Murree, and Nagri) revealed significant variations in mineralogical composition and textural characteristics that directly influenced their engineering behaviour. The modal composition analysis of the investigated sandstone samples has been carried out through the visual estimation technique (Table 2). The Chichali Formation (CF) is composed of quartz (53 %), alkali feldspar (5 %), glauconite (35 %), and matrix (5 %) (Table 2). The modal composition of quartz (Q), feldspar (F), and lithic fragments (L) was normalized and plotted on a QFL ternary diagram, where the CF

Table 1 A list of engineering quality tests performed according to standards.

S. No	Names of tests performed	Standards followed
1	Specific gravity and Water absorption	ASTM C 127 (2024)
2	Ultrasonic pulse velocity	Aydin (2014)
3	Schmidt hammer test	ASTM D5873-14 (2014)
4	Unconfined compressive strength	ASTM D 2938-95 (2016)
5	Unconfined tensile strength	ASTM D 3967 (2016)
6	Point load index	ASTM D5731-16 (2016)



Fig. 3 Photographs showing various geotechnical tests. **a)** showing Schmidt hammer test of the bulk samples; **b)** showing Water absorption test of the core samples; **c)** showing Unconfined Compressive Strength test of the core samples; **d)** showing Unconfined Tensile Strength test of the core samples; **e)** showing Point Load Test of the core samples; **f)** showing Ultrasonic Pulse Velocity test of the core samples.

sandstone falls within the compositional field of sub arkose (Fig. 4). Based on the grain size variation and comparison with the Wentworth (1922) grain size scale, CF sands fall in the category of fine silt to very fine sand (Table 3). Texturally the grains are sub-angular to sub-rounded, showing low to moderate sphericity, moderately to well-sorted, and showing straight to concavo-convex contacts (Figs. 5a, b). The CF sandstone is both texturally and compositionally mature.

The Lumshiwai Formation (LF-1) is predominantly of quartz (95 %) and feldspar (5 %) (Table 2). The LF-1 sandstone falls within the compositional field of quartz arenite on the QFL ternary diagram (Fig. 4). Based on the grain size variation, LF-1 sandstone falls in the category of coarse silt to very coarse sand (Table 3). Texturally the grains are sub-rounded to rounded, showing moderate to high sphericity, are poorly to moderately sorted, and exhibit straight, sutured, and concavo-convex contacts

Table 2 Modal composition of the studied sandstone samples.

Sample No.	Modal Composition						Classification (after Pettijohn et al., 1987)	
	Quartz	Feldspar	Lithics	Glauconite	Bioclasts	Muscovite		Matrix
CF	53	5		37			5	Sub arkose
LF-1	95	5						Quartz arenite
LF-2	50			8	17		25	Bioclastic quartz wacke
MF	57	10	30		1	2		Litharenite
NF	35	15	45		1	3		Feldspathic litharenite

Table 3 Textural characteristics of the studied sandstone samples.

Sample No.	Grain size (µm)	Grain shape		Sorting	Packing/contacts	Textural Maturity	Compositional Maturity
		Roundness	Sphericity				
CF	(13.53 - 104.08) Fine silt to very fine sand Average = 48	Sub-angular to sub-rounded	Low to moderate	Moderate to well-sorted	Straight and concavo-convex	Mature	Mature
LF-1	(52.58 - 1610) Coarse silt to very coarse sand Average = 197.65	Sub-rounded to well-rounded	Moderate to high	Poor to moderate	Straight, sutured, and concavo-convex	Mature	Supermature
LF-2	(25.61 - 187.25) Medium silt to fine sand Average = 86.51	Sub-rounded to rounded	Moderate to high	Moderate to well-sorted	Floating, point, straight, and concavo-convex	Immature	Mature
MF	(28.38 - 709) Medium silt to coarse sand Average = 164	Sub-rounded to well-rounded	Moderate to high	Moderate to well-sorted	Straight and concavo-convex	Mature	Mature
NF	(13.37 - 411.77) Fine silt to medium sand Average = 126.40	Sub-rounded to rounded	Low to moderate	Poor to moderate	Straight and concavo-convex	Mature	Immature

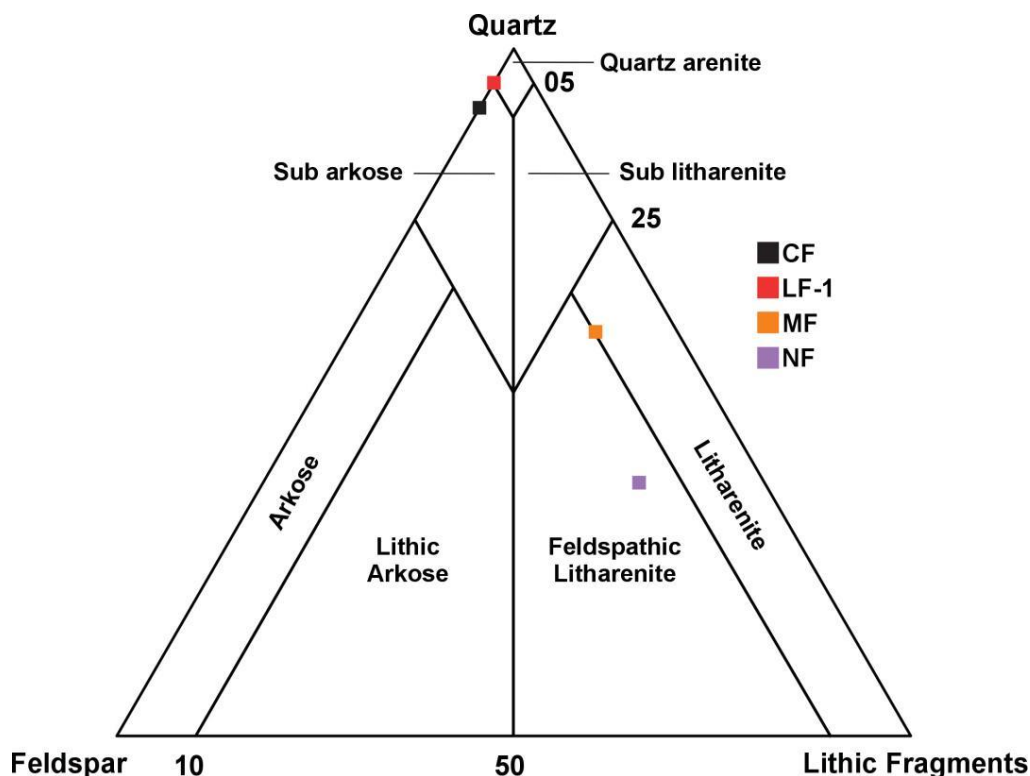


Fig. 4 QFL ternary diagrams for compositional classification of the studied sandstones (after Pettijohn et al., 1987).

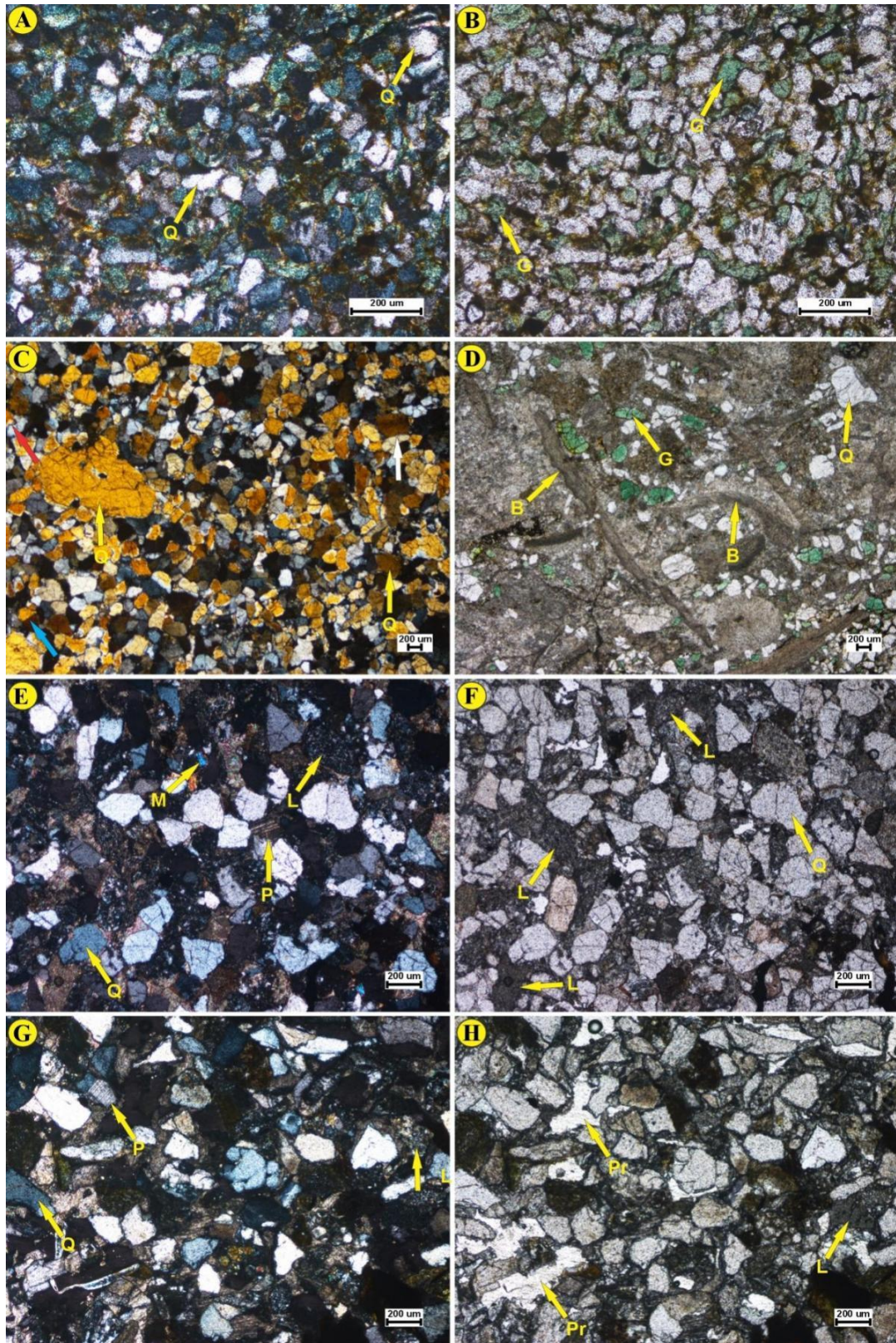


Fig. 5 Petrographic characteristics of the studied sandstone samples. (A: XPL; B: PPL) Quartz (Q) and glauconite (G) in the sub arkose sandstone of the Chichali Formation (Ch). (C: XPL) Dominantly quartz with straight (indicated by blue arrows), concavo-convex (white arrow), and sutured (red arrow) grain boundaries in the quartz arenite of the Lumshiwal Formation (Lsh-1). (D: PPL) Bioclasts (B), glauconite (G), and quartz (Q) in the bioclastic quartz wacke of the Lumshiwal Formation (Lsh-2). (E: XPL; F: PPL) Quartz (Q), plagioclase feldspar (P), lithic fragments (L), and muscovite (M) in the litharenite of the Muree Formation (MF). (G: XPL; H: PPL) Quartz (Q), lithic fragments (L), plagioclase feldspar (P), and porosity (Pr) in the feldspathic litharenite of the Nagri Formation.

(Fig. 5c). The LF-1 sandstone is both physically and chemically mature. The LF-2 sandstone is composed of Quartz (50 %), glauconite (08 %), bioclasts (17 %), and matrix (25 %). The LF-2 sandstone is classified as bioclastic quartz wacke based on the Pettijohn et al. (1987) classification scheme. Based on the grain size variation, LF-2 sandstone falls within the category of medium silt to fine sand (Table 3). Texturally the grains are sub-rounded to rounded, showing moderate to high sphericity, moderate to well-sorted, and showing dominantly floating texture with a minor amount of straight and concavo-convex contacts (Fig. 5d). The LF-2 sandstone is texturally immature due to the high proportion of very fine-grained matrix and chemically mature.

The modal composition of the Murree Formation (MF) is comprised of quartz (57 %), feldspar (10 %), lithic fragments (30 %), bioclasts (01 %), and muscovite (02 %) (Table 2). Feldspar is dominantly comprised of plagioclase. Lithic fragments include undifferentiated very fine-grained textured igneous and metamorphic rock fragments (Fig. 5). The MF sandstone falls within the compositional field of litharenite on the QFL ternary diagram (Fig. 4). Based on the grain size variation, MF sandstone falls in the category of medium silt to coarse sand (Table 3). Texturally the grains are sub-rounded to well-rounded, showing moderate to high sphericity, moderate to well-sorted, and exhibit straight to concavo-convex contacts (Figs. 5e, f). The MF sandstone is both physically and chemically mature.

The modal composition of the Nagri Formation (NF) is composed of quartz (35 %), feldspar (15 %), lithic fragments (45 %), bioclasts (01 %), and muscovite (03 %) (Table 2). Lithic fragments are composed of volcanic and metamorphic rock fragments, contributing to its heterogeneous fabric (Figs. 5g, h). The NF sandstone falls within the compositional field of feldspathic litharenite on the QFL ternary diagram (Fig. 4). Based on the grain size variation, NF sandstone falls in the category of fine silt to medium sand (Table 3). Texturally the grains are sub-rounded to rounded, showing low to moderate sphericity, poorly sorted, and exhibit straight to concavo-convex contacts (Fig. 5). The NF sandstone is both physically and chemically mature.

The EDS analysis reveals the presence of abundant silica, feldspar, clay minerals, and calcite. In addition, SEM-based observations reveal porosity in the Nagri Formation (Fig. 6). The EDS and SEM results support petrographic observations.

4.2. PHYSICAL PROPERTIES

In order to utilize sandstones in engineering projects, it is essential to evaluate their physical and mechanical properties through various physical tests. The outcomes of the physical tests presented in Table 4 reveal that the quartz arenite sandstone from Lumshiwal Formation showed the highest specific gravity (average 2.94), consistent with its dense

quartz-rich composition and minimal porosity (0.26). The low (0.11 %) water absorption values are reflecting the well-cemented nature of these sandstones. The sandstone from Murree Formation exhibited the average specific gravity as 2.74 and the average water absorption as 0.13 %. The sandstone from Chichali Formation showed a reduction in specific gravity (2.61) and higher water absorption (0.16 %) which can be correlated with its glauconite content and moderate porosity (0.32). Similarly, the bioclastic quartz wacke sandstone of Lumshiwal Formation displayed even lower specific gravity (2.56) and higher water absorption (0.20 %), consistent with its bioclast-rich and porous fabric. The sandstone of Nagri Formation exhibited the lowest specific gravity (2.49) and the highest water absorption (0.24 %), directly reflecting its high porosity (0.43) and weak cementation.

4.3. MECHANICAL PROPERTIES

The results of mechanical properties of the sandstone of various formations of the study area are presented in Table 4. The results obtained through the unconfined compressive strength testing of the studied sandstones are very well correlated with their mineralogical composition and textural characteristics. The quartz arenite sandstone facies of the Lumshiwal Formation demonstrated exceptional strength (average UCS 145 MPa). This performance reflects the combined effects of high quartz content, strong silica cementation, and minimal porosity. Unconfined tensile strength tests yielded similarly high values (19 MPa), while point load testing showed consistent results (23 MPa). The sandstone of the Murree Formation demonstrated an average UCS of 105 MPa. This performance is attributed to its predominantly quartz-rich composition, higher quartz-to-feldspar ratio, and lower porosity. Tensile strength (15 MPa) and point load strength (20 MPa) followed similar trends, while ultrasonic pulse velocity measurements (4601 m/s) and Schmidt hammer rebound values (41) further confirmed its higher mechanical properties.

The sandstone from Chichali Formation showed reduced strength (UCS 93 MPa), with glauconite content and moderate porosity contributing to its decreased mechanical performance. Tensile strength (12 MPa) and point load strength (16 MPa) were relatively lower, while UPV (4065 m/s) and Schmidt hammer values (34) reflected this reduced competence.

The mechanical properties (UCS 74 MPa) of the bioclastic quartz wacke sandstone facies from the Lumshiwal Formation were significantly influenced by its high bioclast and calcareous content and porosity. The weak carbonate-cemented fabric resulted in lower tensile strength (8 MPa) and point load strength (12 MPa). The UPV measurements (2908 m/s) and Schmidt hammer values (29) also demonstrated their lower mechanical performance.

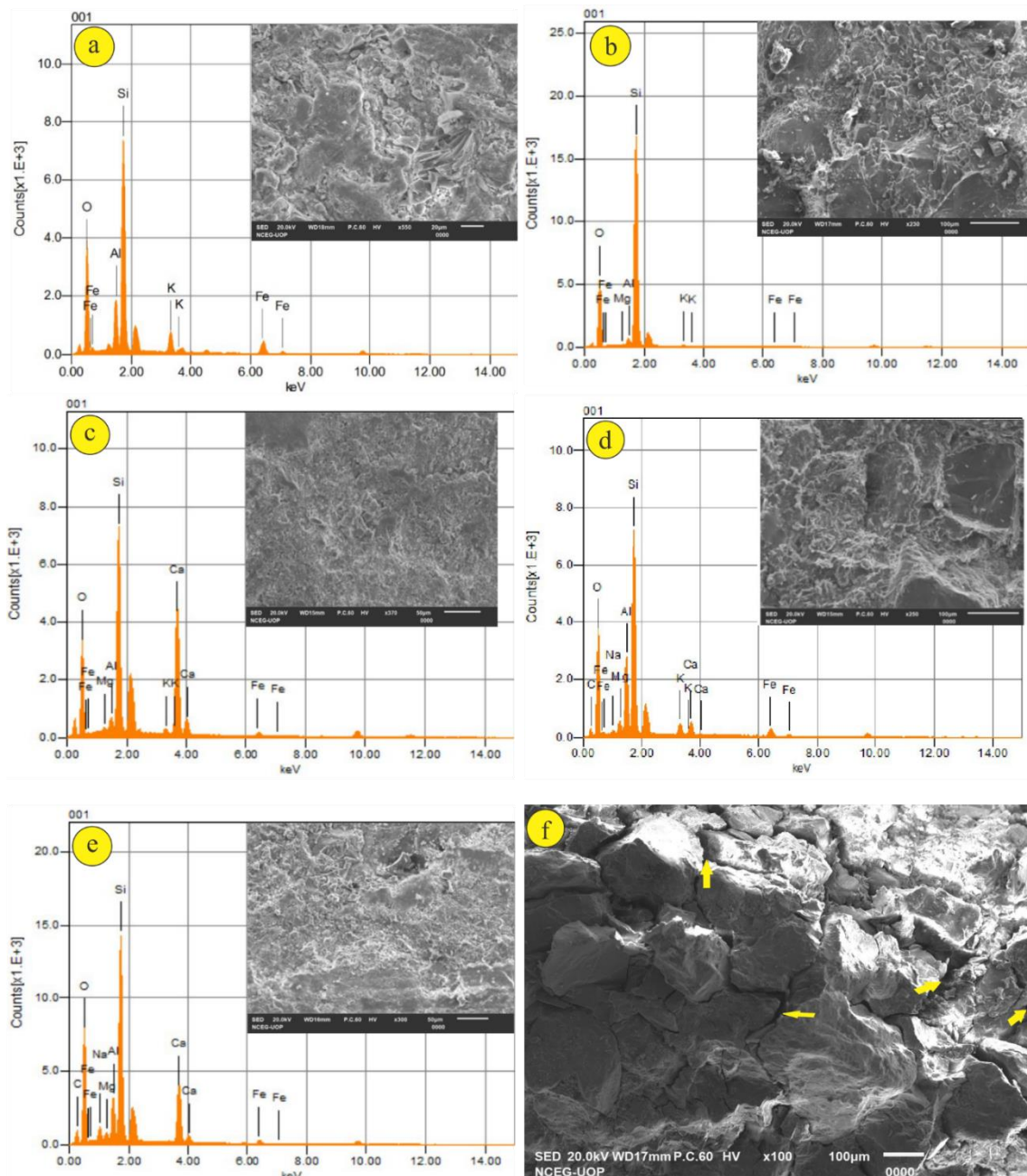


Fig. 6 EDS plots illustrating the elemental composition of the studied formations. (a) Elemental composition of the subarkose sandstone from the Chichali Formation; (b) Quartz-arenite of the Lumshiwal Formation; (c) Bioclastic quartz wacke of the Lumshiwal Formation; (d) Litharenite of the Murree Formation; (e) Elemental composition of the feldspathic litharenite from the Nagri Formation; (f) Yellow arrows indicating porosity in the Nagri Formation.

The Sandstone of the Nagri Formation displayed the poorest mechanical performance (UCS 63 MPa), directly attributable to its high feldspar content, higher porosity, and weak cementation. Tensile strength was remarkably low (5 MPa), with point load tests yielding minimal values (7 MPa). The UPV (2140 m/s) and Schmidt hammer rebound (23) were correspondingly reduced, confirming its marginal engineering suitability.

5. DISCUSSION

5.1. RELATIONSHIP BETWEEN THE QUARTZ CONTENT AND MECHANICAL STRENGTH

The relationship between mineralogy and mechanical strength, particularly the role of quartz, represents a fundamental question in rock mechanics. Quartz, with its high hardness and strong covalent bonds, is intuitively considered a primary contributor to rock strength. However, the global body of research

Table 4 Geotechnical analysis of the studied sandstone samples.

Formations	Abbr.	Specific gravity	Water absorption	Porosity	UCS (MPa)	UTS (MPa)	PLT	UPV (m/s)	SHT
LF-1	LF-1	2.95	0.09	0.25	156	20	24	6304	50
	LF-2	2.93	0.12	0.27	135	17	21	5380	46
	LF-3	2.95	0.1	0.26	151	19	23	6073	49
	LF-4	2.94	0.12	0.27	140	18	22	5611	47
	LF-5	2.94	0.11	0.26	146	19	23	5842	48
	Ave.	2.94	0.11	0.26	145	19	23	5842	48
MF	M1	2.78	0.11	0.21	120	16	21	4822	44
	M2	2.7	0.14	0.23	90	13	18	4380	38
	M3	2.76	0.12	0.22	113	15	20	4712	43
	M4	2.72	0.14	0.23	98	14	19	4491	40
	M5	2.75	0.13	0.22	105	15	20	4601	41
	Ave.	2.74	0.13	0.22	105	15	20	4601	41
CF	C1	2.62	0.15	0.3	100	13	17	4250	36
	C2	2.6	0.17	0.33	85	10	14	3880	31
	C3	2.62	0.16	0.32	97	12	16	4158	35
	C4	2.61	0.17	0.33	88	11	15	3973	32
	C5	2.61	0.16	0.32	93	12	16	4065	34
	Ave.	2.61	0.16	0.32	93	12	16	4065	34
LF-2	L1	2.6	0.18	0.35	80	9	13	3050	31
	L2	2.5	0.22	0.37	68	7	10	2766	27
	L3	2.6	0.19	0.36	77	9	12	2979	30
	L4	2.5	0.21	0.37	71	8	11	2837	28
	L5	2.6	0.2	0.36	74	8	12	2908	29
	Ave.	2.56	0.2	0.36	74	8	12	2908	29
NF	N1	2.55	0.22	0.41	70	6	9	2390	25
	N2	2.43	0.25	0.44	55	4	5	1890	20
	N3	2.52	0.23	0.42	66	6	8	2265	24
	N4	2.46	0.24	0.43	59	5	6	2015	21
	N5	2.49	0.24	0.43	63	5	7	2140	23
	Ave.	2.49	0.24	0.43	63	5	7	2140	23

presents a paradox. A multitude of studies corroborate this intuition, reporting strong positive correlations between quartz content and compressive strength in various sandstone types and crystalline rocks (e.g., Tuğrul and Zarif, 1999; Yesiloglu-Gultekin et al., 2013; Sajid and Arif, 2015). These findings affirm quartz's role as a rigid framework builder that enhances resistance to weathering and mechanical stress.

In stark contrast, an equally credible set of studies complicates this narrative. Some researchers argue that the inherent brittleness of quartz can facilitate crack propagation, thereby diminishing overall strength (Sousa, 2013). Perhaps more significantly, several investigations have found no statistically significant correlation, concluding that for certain rock suites, mineral composition is a secondary factor to textural parameters like grain interlocking, cementation, and porosity (e.g., Diamantis et al., 2014; Ündül and Er, 2017; Hemmati et al., 2020). This ongoing debate underscores a critical insight: the influence of quartz is not absolute but is filtered and potentially obscured by the rock's textural maturity and diagenetic history.

Our comprehensive dataset from the Nizampur and Kohat basins cuts through this ambiguity, providing a clear and compelling case for quartz content as the dominant control on strength within this specific geological context. The evidence is both

strong and consistent across all testing methods. Most strikingly, a simple linear regression reveals that quartz percentage alone accounts for a remarkable 94.6 % of the variance in Unconfined Compressive Strength (UCS) (Fig. 7a). The regression equation ($UCS = 0.583 * Quartz \% - 1.116$) provides a powerful predictive tool, with the tight clustering of data points around the trendline underscoring the reliability of this relationship. This finding decisively positions quartz content as the principal determinant of compressive strength for these sandstones.

In contrast, the UTS-quartz relationship, Figure 8b shows a steeper positive trend. The regression line, $y = 3.6667x + 14.833$, indicates a substantial positive trend where UTS increases with higher quartz content. The R^2 value (0.7451) reflects a strong, though not perfect, linear relationship, explaining about 74.5 % of the variability in UTS. Data points are labeled with sample identifiers (LF-1, CF, MF, NF, LF-2), showing some spread around the trendline. While not as robust as the UCS-Quartz relationship, this still demonstrates quartz's significant influence on tensile strength. The steeper slope (3.6667 vs. 0.583 in the UCS graph) suggests quartz content has a more pronounced effect on UTS than on UCS per percentage point.

Nonetheless, Merriam et al. (1970) reported an inverse relationship. Moreover, Hemmati et al. (2020) and Příkryl (2001) did not find any relationship

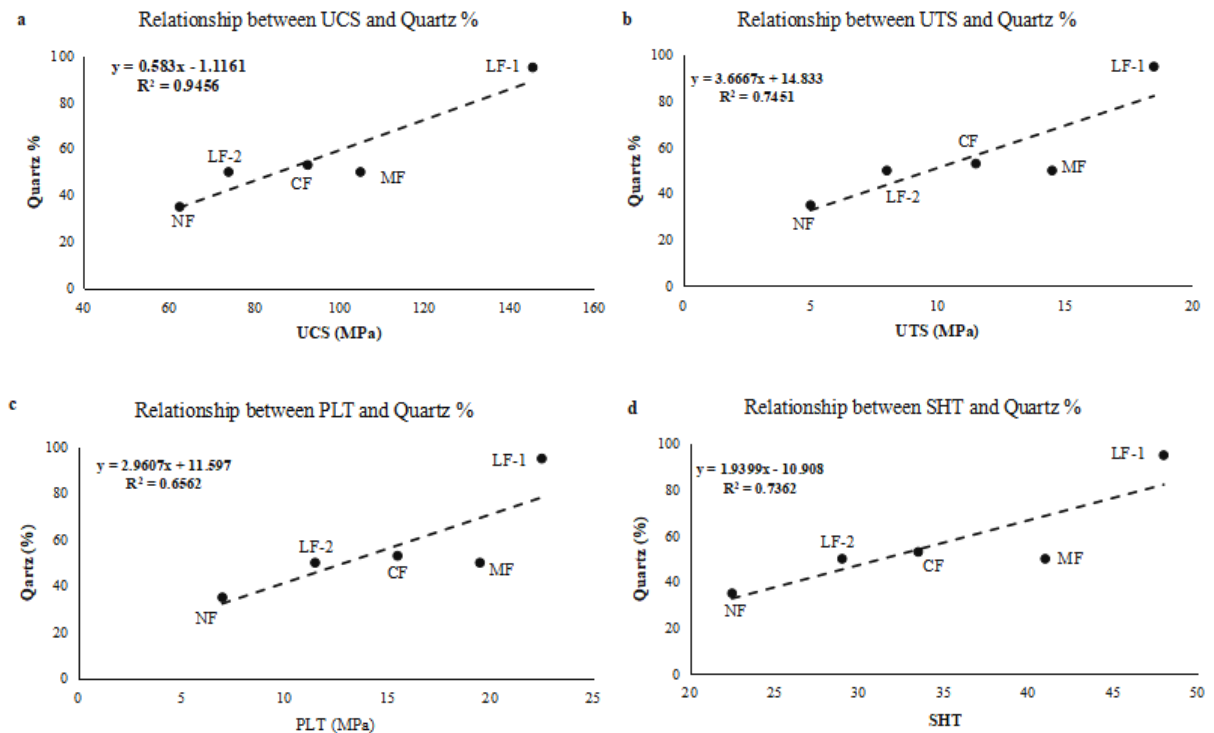


Fig. 7 The relationship between quartz percentage and the engineering properties of the studied samples.

between the quartz content and the tensile strength of the rock. The reason for contradictory results in this field may be the result of different origins of the rock specimens. Based on the results obtained in this research, it is clear that for rocks with a limited number of minerals, the percentage of quartz is an indicator for determining the mechanical properties. Meanwhile, the brittleness reduces tensile strength because it harms tensile strength. The bond between quartz and other minerals can affect the rock's tensile strength. A weak bond can reduce the tensile strength, while a strong bond can increase it. Otherwise, the textural characteristics of rocks are likely the main cause of this issue.

The scatter plot (Fig. 7c) illustrates the relationship between PLT strength and quartz percentage in studied samples. The fitted regression line, given by the equation $y = 2.9607x + 11.597$, demonstrates a positive linear trend, suggesting that PLT strength increases with higher quartz content. The coefficient of determination ($R^2 = 0.6562$) shows that approximately 66% of the variation in quartz percentage can be explained by changes in PLT values. Notably, sample LF-1 exhibits the highest quartz content and PLT value, while NF lies at the lower end of both axes. This plot highlights a moderately strong influence of quartz on the point load strength of sandstone, supporting the interpretation that increased quartz content enhances the rock's resistance to concentrated loading.

The scatter plot (Fig. 7d) illustrates the correlation between SHT rebound values and quartz content (%) in studied sandstones. The regression

equation, $y = 1.9399x - 10.908$, indicates a positive linear relationship, suggesting that as quartz content increases, the SHT values also rises. The R^2 value of 0.7362 signifies a strong correlation, with approximately 73.6% of the variation in rebound strength explained by the quartz percentage. Among the studied samples, LF-1 stands out with the highest quartz content (95%) and the maximum SHT value (48), while sample N, with the lowest quartz content (35%), has the lowest rebound value (23). Intermediate samples (M, C, and LF-2) follow the overall trend with minor deviations. These findings confirm that quartz-rich rocks exhibit higher surface hardness, reinforcing the value of quartz content as a key predictor in non-destructive strength assessments using the Schmidt hammer.

As can be seen in Figure 7d, the L-type Schmidt hammer rebound number (R) will increase with an increase in quartz content. Note that R is defined as the distance travelled by the piston after the rebound. This is considered to be an index of surface hardness that corresponds with the UCS of various rocks (Aydin and Basu, 2005). Quartz mineral has a hardness of 7 on the Mohs scale, which is higher than many other rock-forming minerals. Quartz minerals can better resist the penetration of the Schmidt hammer piston, leading to a penetration resistance (or hardness) of the mineral surface and quick piston rebound. Therefore, shorter penetration time or depth justifies lesser work or energy loss and a greater rebound number. The results of this research indicate a direct linear relationship with a good correlation coefficient between quartz content and rebound number (Fig. 7).

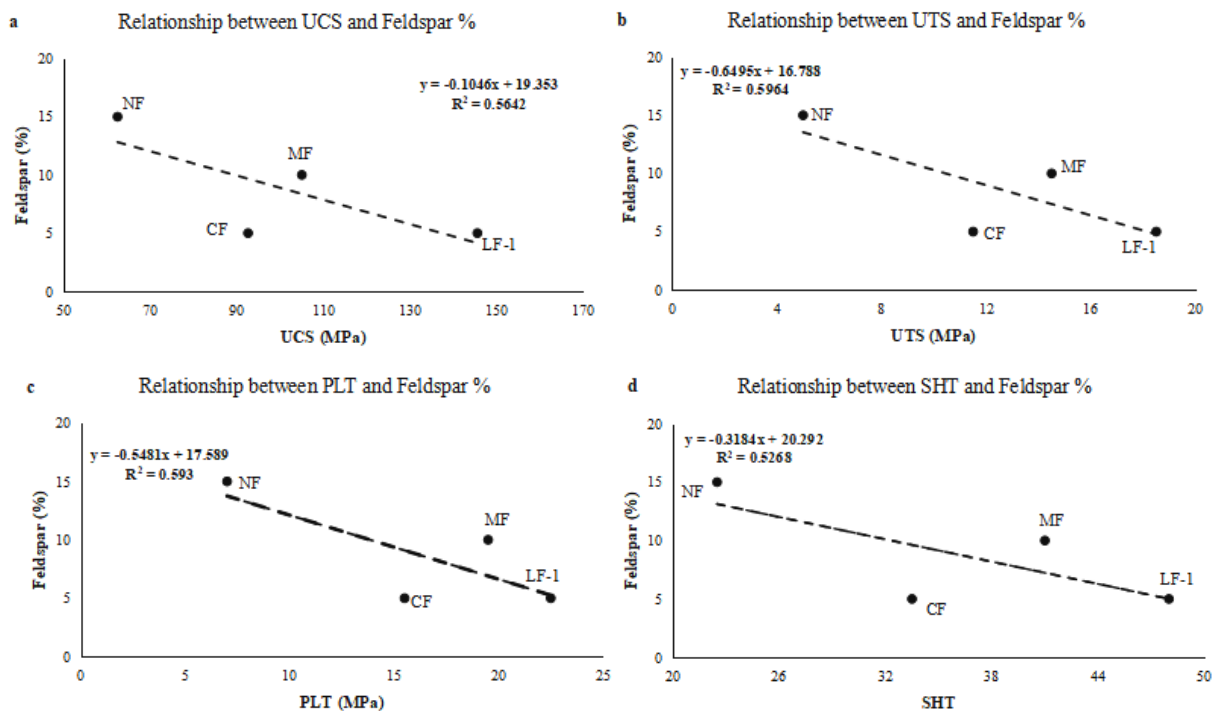


Fig. 8 The relationship between feldspar percentage and the engineering properties of the studied sandstone samples.

5.2. RELATIONSHIP BETWEEN THE PERCENTAGE OF FELDSPAR AND THE MECHANICAL PROPERTIES OF ROCKS

The relationship between feldspar content and mechanical properties of all rock specimens is illustrated in Figure 8. The relationship between UCS and the percentage of feldspar in the tested samples have been shown Figure 8a. A linear regression line, defined by the equation $y = -0.1046x + 19.353$, is fitted to the data, indicating a very slight negative trend where UCS marginally decreases as feldspar percentage increases. However, the low R^2 value (0.5642) suggests that this trend is statistically weak, meaning feldspar content has minimal influence on UCS. The data points, labeled MF, NF, LF-2, CF, and LF-1, are widely scattered, further emphasizing the lack of a strong correlation. UCS values vary significantly, ranging from approximately 20 to 140 MPa, but no clear pattern emerges based on feldspar content.

The scatter plot (Fig. 8b) examines the connection between UTS and feldspar percentage. The regression line, $y = -0.6495x + 16.788$, shows a gentle downward slope, proposing a minor decrease in UTS with higher feldspar content. However, the R^2 value (0.5964) is exceptionally low, indicating that the linear model poorly explains the data variability. Data points are labeled LF-2, CF, and LF-1, with UTS values clustered between roughly 2 and 6 MPa. The near-zero R^2 and tight clustering suggest that feldspar percentage has negligible predictive power for UTS in this dataset.

The scatter plot (Fig. 8c) explores the relationship between PLT values and feldspar content (%) in sandstone samples. The regression equation, $y = -0.5481x + 17.589$, indicates a slight negative trend, suggesting that an increase in feldspar content may lead to a decrease in PLT values. However, the very low R^2 value (0.593) reveals that feldspar content has virtually no explanatory power for the variability in PLT strength. For instance, sample M, despite having the highest feldspar content (40%), retains a relatively high PLT value (20), while sample N, with 30% feldspar, shows the lowest PLT value (7). Conversely, samples LF-1 and C exhibit high PLT values (23 and 16) with very low feldspar content (5%). These inconsistencies highlight a weak and unreliable relationship, suggesting that feldspar percentage is not a significant predictor of point load strength in these sandstone samples.

The graph (Fig. 8d) explores the impact of feldspar content on SHT. The regression equation, $y = -0.3184x + 20.292$, implies a weak negative trend, but the R^2 value (0.5268) confirms almost low linear relationship. Data points are marked as MF, LF-2, CF, and LF-1, with SHT values distributed across a broad range (0–50). The high scatter plot and near-zero R^2 reinforce that feldspar percentage does not meaningfully influence SHT in these samples.

Our analysis demonstrates that feldspar content is not a statistically significant predictor of mechanical strength in the studied sandstones (Fig. 8). The consistently low R^2 values across all mechanical tests confirm that variations in feldspar percentage explain

very little of the observed strength variability, underscoring the primacy of quartz content in this geological context (Sajid et al., 2016), it does not appear to be a significant determinant of mechanical strength in the specific samples analyzed (Asif et al., 2024).

5.3. RELATIONSHIP BETWEEN THE QUARTZ-TO-FELDSPAR RATIO AND THE MECHANICAL PROPERTIES OF ROCKS

Phase ratio analysis was first used by Tuğrul and Zarif (1999) to investigate the relationship between mineral content ratio and resistance properties. They showed that the QFR can be positively correlated with the compressive and tensile strength of rocks. Several positive results (Hajiabdolmajid and Kaiser, 2002), negative results (Sousa, 2013) and results without effect (GüneşYilmaz et al., 2011; Hemmati et al., 2020) have been reported regarding the hypothesis of the relationship between the QFR ratio and rock strength. This apparent contradiction is most likely due to different mineralogical compositions of the studied samples. From the point of view of lithology, all samples used by researchers such as Tuğrul and Zarif (1999) may have quartz content ranging from 10 % to 33 %, while other researchers used samples containing different minerals and with higher quartz proportions.

The relationship between the QFR ratio and the UCS of this research is presented in Figure 9a. The graph demonstrates a moderately strong positive correlation between UCS and the QFR. The regression line, defined by the equation $y = 0.1894x - 9.9671$, indicates that UCS increases as the QFR ratio rises. The R^2 value of 0.7814 suggests that approximately 78.1 % of the variability in UCS can be explained by this ratio, indicating a meaningful but not exhaustive relationship. Data points are labeled with sample identifiers (LF-1, CF, NF, MF), showing some scatter around the trendline. UCS values range up to ~160 MPa, with the ratio's influence becoming more pronounced at higher values. This graph implies that a higher proportion of quartz relative to feldspar enhances compressive strength, though other factors likely contribute to the remaining variability. Recent research by Yusof and Zabidi (2016), Hemmati et al. (2020), Ahmad et al. (2021) and Heydarian et al. (2024) is in good agreement with the results obtained in this research. It is noticed that the significance of the QFR is essentially limited by the minimum percentage of quartz present in the rocks, while the best results are obtained for quartz-rich specimens (Hemmati et al., 2020). Also, another reason for reducing the importance of this ratio could be the degree of alteration of feldspar.

The relationship between the QFR and the UTS is a direct linear trend that is similar to the trend for compressive strength (Fig. 9b). This relationship does not agree with the results obtained by Yusof and Zabidi (2016) because they did not find any relationship between these two parameters. However, Tuğrul and Zarif (1999), Hemmati et al. (2020) and

Heydarian et al. (2024) observed a very good agreement and reported a direct relationship with a strong correlation coefficient between these two parameters. The reason for the difference in compressive and tensile strength characteristics may be the different types of feldspars. The mechanical behavior of feldspar minerals varies based on the frequency of existing structural discontinuities such as cleavage surfaces or microcracks. This ultimately results in different mechanical characteristics. Plagioclases are expected to have inferior mechanical properties because they contain many more planes of weakness (cleavage and microcracks) compared with other feldspars, such as alkali feldspars (orthoclase and sanidine). This is due to weakly bounded cleavage planes, which promote tensile failure. Plagioclase typically contains well-defined mineral cleavages that function as additional weak planes that facilitate crack propagation all through grains. It is well established that when a specimen is loaded, fractures often follow preferred directions, such as grain boundaries and mineral cleavage planes in rock material (GüneşYilmaz et al., 2011).

The scatter plot (Fig. 9b) examines the connection between UTS and the QFR. The regression line, $y = 1.0343x - 3.5656$, shows a steeper positive slope compared to the UCS graph, suggesting a more dramatic increase in UTS per unit increase in the ratio. However, the R^2 value of 0.6386 indicates that only about 63.8 % of the variability in UTS is explained by the ratio, leaving room for other influencing factors. Data points labeled LF-1, CF, NF, MF exhibit noticeable scatter, particularly at lower ratios. The trend implies that quartz-rich compositions improve tensile strength, but the effect is less predictable than for UCS.

Figure 9c explores the link between PLT strength and the QFR ratio. The regression line, $y = 0.8113x - 3.8489$, suggests a positive trend, but the R^2 value of 0.5486 reveals that only 54.8 % of PLT variability is tied to this ratio. Data points (labeled LF-1, CF, NF, MF) are widely dispersed, especially at lower ratios. PLT values cap at ~20 MPa, with the trendline indicating that higher quartz content relative to feldspar modestly improves point load strength. The lower R^2 suggests PLT is less dependent on this ratio compared to UCS or UTS.

Regarding the relationship between the QFR and the Schmidt hammer rebound number, a direct correlation can be seen between the two parameters. This means that with an increase in minerals resistant to physical and chemical weathering, the Schmidt hammer rebound number will increase. The Figure 9d analyzes SHT against the QFR. The regression line, $y = 0.52x - 9.6163$, shows a positive but weak trend, with an R^2 of 0.5934, explaining only 59.3 % of SHT variability. Samples (LF-1, CF, MF) highlight sample-specific deviations, particularly for MF. The negative intercept suggests negligible SHT at very low quartz ratios. Like PLT, SHT's dependence on the ratio is discernible but overshadowed by other factors.

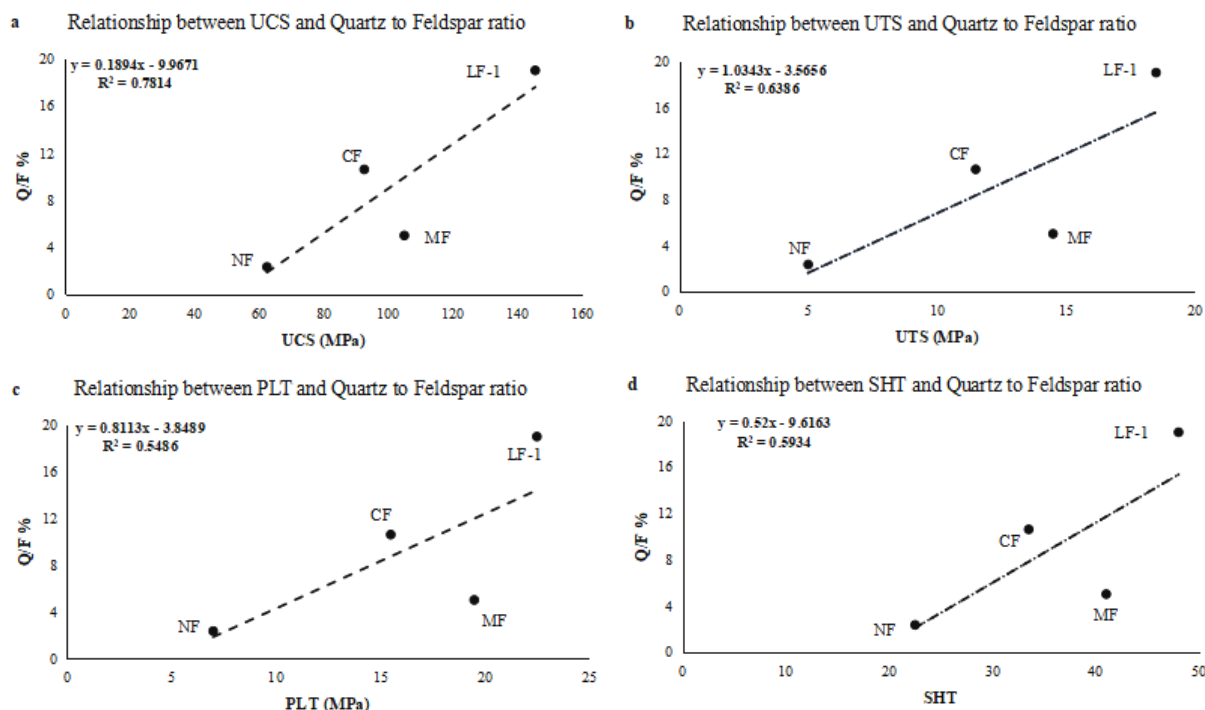


Fig. 9 The relationship between the quartz-to-feldspar ratio and the engineering properties of the studied sandstone samples.

5.4. RELATIONSHIP BETWEEN TEXTURAL CHARACTERISTICS AND STRENGTH PROPERTIES

Apart from the influence of mineralogical composition, the textural characteristics also play a significant role in determining the engineering properties of sandstone rocks. For the quartz arenite of the Lumshiwai Formation, the exceptional strength is directly attributable to its high textural and compositional maturity, with a tightly packed, interlocking fabric characterized by straight, concavo-convex, and sutured contacts, which effectively dissipates stress and inhibits crack propagation. Similarly, the high strength of the sandstone from the Murree Formation can be ascribed to the same reasons (Fig. 5). In contrast, the bioclastic quartz wacke of the Lumshiwai Formation exhibits weak strength due to its compositional immaturity and a "floating" texture where grains are not load-bearing, leading to premature failure. Similarly, the sandstone of the Nagri Formation shows low strength, which is directly linked to poor sorting, compositional immaturity, and high porosity, which collectively create a heterogeneous fabric with abundant pre-existing pathways for crack initiation and growth (Figs. 5, 6).

The strong correlations established in this study have direct practical implications for field engineering. A field engineer can use a simple Schmidt hammer test to obtain a rapid, non-destructive estimate of a sandstone's strength potential. For instance, a rebound value (R) above 40 strongly indicates a high-quartz, high-strength rock (UCS > 100 MPa) suitable for major structural work, like the Lumshiwai quartz arenite. Conversely, a value below 30 suggests a weaker, more porous sandstone, like the

Nagri Formation, which may be suitable only for backfill or non-critical applications. Furthermore, a basic visual petrographic assessment estimating a high quartz content (e.g., >70 %) can serve as a preliminary, qualitative indicator of good mechanical performance, allowing for rapid initial site assessments and material selection before undertaking more expensive and time-consuming laboratory tests.

6. CONCLUSIONS

This study investigated the mineralogical and textural influences on the physical and mechanical properties of sandstones from the Nizampur and Kohat basins in Pakistan. The results demonstrate a strong positive correlation between quartz content and mechanical strength, with quartz-rich sandstones (e.g., Lumshiwai Formation) exhibiting the highest compressive and tensile strength due to their strong covalent bonds and resistance to weathering. In contrast, feldspathic litharenite (e.g., Nagri Formation) displayed the weakest mechanical performance, attributed to high porosity, poor sorting, and compositional immaturity.

Textural characteristics, including grain packing, sorting, and porosity, significantly influenced strength. Tightly packed grains with sutured and concavo-convex contacts enhanced mechanical properties, whereas poorly sorted, porous textures reduced them. Non-destructive tests (SHT, UPV) proved effective in assessing strength, correlating well with quartz content, thus offering practical field evaluation methods.

These findings provide crucial insights for selecting suitable sandstone units in construction and geotechnical projects. Future research should explore

microfracture propagation, advanced numerical modeling, and long-term weathering effects to further refine engineering applications. This study fills a critical gap in understanding Pakistani sandstones, contributing to more informed material selection and construction practices. The correlations established here provide a foundation for developing a regional geotechnical classification system for construction materials. Future work should focus on microfracture propagation under load using advanced imaging techniques, numerical modeling to simulate the failure of these heterogeneous materials, and long-term durability studies assessing the impact of weathering on these mechanical relationships.

ACKNOWLEDGMENTS

The authors would like to acknowledge the National Centre of Excellence in Geology at the University of Peshawar, Pakistan, for providing essential laboratory facilities and field logistics.

AUTHOR CONTRIBUTION

Sajjad Ahmad, contributed to conceptualization, methodology, field investigation, data curation, and writing original draft; Muhammad Tahir Shah, Muhammad Sajid, Abdul Rahim Asif, Subhan Ullah, and Muhammad Rizwan contributed to reviewing and editing, supervision, and funding acquisition; and Syed Irfanullah Hashmi, Shehzad Mussawar, Syed Saddam Hussain, and Hafiz Shahid Hussain contributed to field investigation, laboratory work, and data support.

FUNDING

Not applicable.

DATA AVAILABILITY

All data are included in the manuscript.

DECLARATION

CONFLICT OF INTEREST

The authors declare that they have no known competing financial interests or personal relationships that could have appeared to influence the work reported in this paper.

REFERENCES

- Ahmad, T., Rizwan, M., Hussain, Z., Ullah, S., Ali, Z., Khan, A., ... and Khan, H.A.: 2021, Mineralogical and textural influence on Physico-Mechanical Properties of selected Granitoids from Besham Syntaxis, Northern Pakistan. *Acta Geodyn Geomater.*, 18, 3. DOI: 10.13168/AGG.2021.0024
- Asif, A.R., Islam, I., Ahmed, W., Sajid, M., Qadir, A. and Ditta, A.: 2022, Exploring the potential of Eocene carbonates through petrographic, geochemical, and geotechnical analyses for their utilization as aggregates for engineering structures. *Arab. J. Geosci.*, 15, 11, 1105. DOI: 10.1007/s12517-022-10383-0
- Asif, A.R., Sajid, M., Ahmed, W. and Nawaz, A.: 2024, Weathering effects on granitic rocks in North Pakistan: petrographic insights, strength classifications, and construction suitability. *Environ. Earth Sci.*, 83, 11, 351. DOI: 10.1007/s12665-024-11655-6
- Asif, A.R., Sajid, M., Ahmed, W., Islam, I., Nawaz, A. and Khattak, S.A.: 2025, Thermal Thresholds and Mechanical Behavior of Granitic Rocks from Northern Pakistan: Implications for Rock Engineering. *Geot Geol Eng*, 43(7), 1–33. DOI: 10.1007/s10706-025-03311-y
- Askari-pour, M., Saeidi, A., Mercier-Langevin, P. and Rouleau, A.: 2022, A review of relationship between texture characteristic and mechanical properties of rock. *Geotechnics.*, 2, 1, 262–296. DOI: 10.3390/geotechnics2010012
- Aydin, A. and Basu, A.: 2005, The Schmidt hammer in rock material characterization. *Eng Geol.*, 81, 1–14. DOI: 10.1016/j. enggeo.2005.06.006
- Barbour, T.G., Atkinson, R.H. and Ko, H.Y.: 1979, Relationship of mechanical, index and mineralogical properties of coal measures rock. Paper presented at the 20th US Symposium on Rock Mechanics, 4–6 June, Austin, TX, 189–198. <https://onepetro.org/ARMAUSRMS/proceedings-abstract/ARMA79/All-AR MA79/ARMA-79-0189/129036>
- Bell, F.G.: 1978, The physical and mechanical properties of Fell Sandstone, Northumberland, England. *Eng Geol*, 12, 1–29.
- Diamantis, K., Gartzos, E. and Migiros, G.: 2014, Influence of petrographic characteristics on physico-mechanical properties of ultrabasic rocks from central Greece. *Bull. Eng. Geol. Environ.*, 73, 4, 1273–1292. DOI: 10.1007/s10064-014-0584-x
- Güneş Yılmaz, N., Mete Goktan, R. and Kibici, Y.: 2011. Relations between some quantitative petrographic characteristics and mechanical strength properties of granitic building stones. *Int. J. Rock Mech. Min. Sci.*, 48, 506–513. DOI: 10.1016/j.ijrmms.2010.09.003
- Hajiabdolmajid, V. and Kaiser, P.: 2002, Brittleness of rock and stability assessment in hard rock tunneling. *Tunn Undergr Space.*, 18, 35–48. DOI: 10.1016/S0886-7798(02)00100-1
- Hashmi, S. I., Jan, I. U., Khan, S. and Ali, N.: 2018, Depositional, diagenetic and sequence stratigraphic controls on the reservoir potential of the Cretaceous Chichali and Lumshiwai formations, Nizampur Basin, Pakistan. *JHES.*, 51, 2, 44–65.
- Hylland, M.D., Riaz, M. and Ahmad, S.: 1988, Stratigraphy and structure of the southern Gandghar range, Pakistan. *JHES*, 21(1), 1–14.
- Hemmati, A., Ghafoori, M., Moomivand, H. and Lashkaripour, G.R.: 2020, The effect of mineralogy and textural characteristics on the strength of crystalline igneous rocks using image-based textural quantification. *Eng Geol.*, 266, 105467. DOI: 10.1016/j. enggeo.2019.105467
- Heydarian, P., Asef, M.R., Hamidi, J.K. and Talkhablo, M.: 2024, The relationship between mechanical properties and mineralogical composition of some sedimentary rocks. *Q. J. Eng. Geol. Hydrogeol.*, 57, 4. DOI: 10.1144/qjegh2024-069
- Hylland, M.D., Riaz, M. and Ahmad, S.: 1988, Stratigraphy and structure of southern Ghandghar Range, Pakistan. *Geol. Bull. Univ. Peshawar.*, 1, 15–24.

- Meissner, C.R., Master, J.M., Rashid, M.A. and Hussain, M.: 1974, Stratigraphy of the Kohat Quadrangle, Pakistan. *Geol. Surv. Prof. Pap.*, 716-D, 37 pp.
- Merriam, R., Rieke III, H.H. and Kim, Y.C.: 1970, Tensile strength related to mineralogy and texture of some granitic rocks. *Eng Geol.*, 4, 2, 155–160. DOI: 10.1016/0013-7952(70)90010-4
- Naseer, S., Ahmad, D. and Hussain, Z.: 2019, Petrographic, Physical and Mechanical Properties of Sandstone of Mirpur District Area State of AJ&K, Pakistan. *ESMY.*, 3, 2, 32–38. DOI: 10.26480/esmy.02.2019.32.38
- Nawaz, A., Sajid, M., Ahmed, W., Asif, A.R. and Ishaq, M.: 2025a, Impact of petrographic and physico-mechanical properties on aggregate suitability of the early Devonian Nowshera formation: a case study from the Peshawar Basin, Pakistan. *Carbonat Evaporit.*, 40, 2, 1–24. DOI: 10.1007/s13146-025-01075-3
- Nawaz, A., Sajid, M., Ahmed, W. and Asif, A.R.: 2025b, Freeze-thaw-induced microstructural alterations and deterioration of physico-mechanical properties in rocks from the Himalayan ranges (Pakistan). *Earth Sci. Res. J.*, 29, 1, 69–80. DOI: 10.15446/esrj.v29n1.116550
- Nawaz, A., Sajid, M., Ahmed, W., Asif, A.R., Alshehri, F., Almadani, S., Shahab, M., Amin, M., Afzal, M.A.: 2025c, Thermal and freeze-thaw-induced degradation of limestone: A comprehensive study on physico-mechanical properties. *Acta Geodyn. Geomater.*, 2 (218), 219–232. DOI: 10.13168/AGG.2025.0015
- Nawaz, A., Sajid, M., Ahmed, W. and Asif, A.R.: 2025d, Thermal degradation of diverse rock suites: Insights from fractures and physical and mechanical analysis. *Rud.-geol.-naft. zb.*, 40(4), 45–56.
- Ozturk, C.A., Nasuf, E. and Kahraman, S.: 2014, Estimation of rock strength from quantitative assessment of rock texture. *J. South. Afr. Inst. Min. Metall.*, 114(6), 471–480.
- Pettijohn, F.J., Potter, P.E. and Siever, R.: 1987, Introduction and source materials. In *Sand and sandstone*, 1–21. New York, NY: Springer New York.
- Přikryl, R.: 2001, Some microstructural aspects of strength variation in rocks. *Int. J. Rock Mech. Min. Sci.*, 38, 671–682. DOI: 10.1016/S1365-1609(01)00031-4
- Sajid, M. and Arif, M.: 2015, Reliance of physico-mechanical properties on petrographic characteristics: consequences from the study of Utlá granites, north-west Pakistan. *Bull. Eng. Geol. Environ.*, 74, 4, 1321–1330. DOI: 10.1007/s10064-014-0690-9
- Sajid, M., Coggan, J., Arif, M., Andersen, J. and Rollinson, G.: 2016, Petrographic features as an effective indicator for the variation in strength of granites. *Eng Geol.*, 202, 44–54. DOI: 10.1016/j.enggeo.2016.01.001
- Shah, S.M.: 2009, Stratigraphy of Pakistan: Ministry of petroleum and natural resources of Geological Survey of Pakistan. *Karachi* 22, 240–256.
- Shakoor, A. and Bonelli, R.E.: 1991, Relationship between petrographic characteristics, engineering index properties, and mechanical properties of selected sandstones. *Bull. Assoc. Eng. Geol.*, 28, 1, 55–71.
- Sousa, L.M.: 2013, The influence of the characteristics of quartz and mineral deterioration on the strength of granitic dimensional stones. *Environ. Earth Sci.*, 69, 4, 1333–1346.
- Tamrakar, N.K., Yokota, S. and Shrestha, S.D.: 2007, Relationships among mechanical, physical and petrographic properties of Siwalik sandstones, Central Nepal Sub-Himalayas. *Eng Geol.*, 90, 3-4, 105–123. DOI: 10.1016/j.enggeo.2006.10.005
- Tuğrul, A. and Zarif, I.H.: 1999, Correlation of mineralogical and textural characteristics with engineering properties of selected granitic rocks from Turkey. *Eng Geol.*, 51, 4, 303–317. DOI: 10.1016/S0013-7952(98)00071-4
- Ullah, S., Sajid, M., Latif, K., Asif, A.R., Rizwan, M., Mussawar, U. and Ullah, S.: 2025, Investigation of depositional fabric and its impact on the geomechanical behavior of limestones. *Carbonat Evaporit.*, 40, 1, 6. DOI: 10.1007/s13146-024-01040-6
- Ündül, Ö. and Er, S.: 2017, Investigating the effects of micro-texture and geo-mechanical properties on the abrasiveness of volcanic rocks. *Eng Geol.*, 229, 85–94. DOI: 10.1016/j.enggeo.2017.09.022
- Waqar, M.F., Guo, S., Qi, S., Karim, M.A.M., Zada, K., Ahmed, I. and Shang, Y.: 2025, Influence of Mineralogical and Petrographic Properties on the Mechanical Behavior of Granitic and Mafic Rocks. *Minerals*, 15(7), 747.
- Wang, W., Huang, J., Chen, D., Luo, Q. and Yuan, B.: 2025, The Effect of Cementation on Microstructural Evolution and Particle Characteristics of Calcareous Sand Under Triaxial Loading. *Buildings*, 15(12), 2041. DOI: 10.3390/buildings15122041
- Wentworth, C. K.: 1929, Method of computing mechanical composition types in sediments. *Geol. Soc. Am. Bull.*, 40, 4, 771–790.
- Williams, H., Turner, F.J. and Gilbert, C.M.: 1982, Petrography an introduction to the study of rocks in thin section Second Edition. WH Freeman and Co., San Francisco, 626 pp.
- Yaseen, M., Shahab, M., Ahmad, Z., Khan, R., Shah, S.F.A. and Naseem, A.A.: 2021, Insights into the structure and surface geology of balanced and retrodeformed geological cross sections from the Nizampur Basin, Khyber Pakhtunkhwa, Pakistan. *J. Pet. Explor. Prod. Technol.*, 11, 2561–2571. DOI: 10.1007/s13202-021-01180-8
- Yasin, M.: 2017, Diagenesis of Miocene Sandstone in the District Sudunhoti and Poonch, Azad Jammu and Kashmir, Pakistan, Pakistan. *J. Geol.*, 1, 1, 5–7.
- Yesiloglu-Gultekin, N., Sezer, E.A., Gokceoglu, C. and Bayhan, H.: 2013, An application of adaptive neuro fuzzy inference system for estimating the uniaxial compressive strength of certain granitic rocks from their mineral contents. *Expert Syst. Appl.*, 40, 3, 921–928.
- Yusof, N.Q.A.M. and Zabidi, H.: 2016, Correlation of mineralogical and textural characteristics with engineering properties of granitic rock from Hulu Langat, Selangor. *Procedia chem.*, 19, 975–980. DOI: 10.1016/j.proche.2016.03.144
- Zhang, Q., Li, Z., Niu, Y., Yin, S., Gao, F., Zhang, F. and Mao, Z.: 2025, The response of electrical potential in sandstone of different sizes under cyclic loading. *Measurement*, 256, part C, 118196. DOI: 10.1016/j.measurement.2025.118196